Supporting Information

Greensporones: Resorcylic Acid Lactones from an Aquatic *Halenospora* sp.

Tamam El-Elimat, Huzefa A. Raja, Cynthia S. Day, Wei-Lun Chen, Steven M. Swanson, and Nicholas H. Oberlies

Tak1–TAB1 (Transforming growth factor–*β* activated kinase–1/TAK–1 binding protein 1) Inhibitor Assays.

Figure S1. UV-PDA spectra of compounds **1**-**14** (200–345 nm)

Figure S2. UPLC chromatograms of compounds **1–11** and **13–14** (λ 254 nm), demonstarting >96% purity for compounds **2–11** and **13–14**, >94% for compound **1,** and >72% for compound **12**. All data were acquired via an Acquity UPLC system with a Phenomenex Kinetex C_{18} (1.3 μm; 50 × 2.1 mm) column and a CH_3CN/H_2O gradient that increased linearly from 20 to 100% CH_3CN over 1.2 min.

Figure S3. ^{1}H and ^{13}C NMR spectra of compound **1** [500 MHz for ^{1}H and 125 MHz for ^{13}C, $CDCl_3$].

Figure S4. ^{1}H and ^{13}C NMR spectra of compound **2** [500 MHz for ^{1}H and 125 MHz for ^{13}C, $CDCl_3$].

Figure S5. ^{1}H and ^{13}C NMR spectra of compound **3** [500 MHz for ^{1}H and 125 MHz for ^{13}C, $CDCl_3$].

Figure S6. ^{1}H and ^{13}C NMR spectra of compound **4** [500 MHz for ^{1}H and 125 MHz for ^{13}C, $CDCl_3$].

Figure S7. ^{1}H and ^{13}C NMR spectra of compound **5** [500 MHz for ^{1}H and 125 MHz for ^{13}C, $CDCl_3$].

Figure S8. ^{1}H and ^{13}C NMR spectra of compound **6** [500 MHz for ^{1}H and 125 MHz for ^{13}C, $CDCl_3$].

Figure S9. ^{1}H and ^{13}C NMR spectra of compound **7** [500 MHz for ^{1}H and 125 MHz for ^{13}C, $CDCl_3$].

Figure S10. ^{1}H and ^{13}C NMR spectra of compound **8** [500 MHz for ^{1}H and 125 MHz for ^{13}C, $CDCl_3$].

Figure S11. ^{1}H and ^{13}C NMR spectra of compound **9** [500 MHz for ^{1}H and 125 MHz for ^{13}C, $CDCl_3$].

Figure S12. ^{1}H and ^{13}C NMR spectra of compound **10** [500 MHz for ^{1}H and 125 MHz for ^{13}C, DMSO].

Figure S13. ^{1}H and ^{13}C NMR spectra of compound **11** [500 MHz for ^{1}H and 125 MHz for ^{13}C, $CDCl_3$].

Figure S14. ^{1}H and ^{13}C NMR spectra of compound **12** [700 MHz for ^{1}H and 175 MHz for ^{13}C, $CDCl_3$].

Figure S15. ^{1}H and ^{13}C NMR spectra of compound **13** [500 MHz for ^{1}H and 125 MHz for ^{13}C, $CDCl_3$].

Figure S16. Stack plot of the ^{1}H NMR spectra of compound **10** (upper), compound **13** (lower) and the rearranged product of compound **10** (middle) [500 MHz, $CDCl_3$].

Figure S17. ^{1}H and ^{13}C NMR spectra of compound **14** [500 MHz for ^{1}H and 125 MHz for ^{13}C, $CDCl_3$].

Figure S18. ^{1}H NMR spectrum of compound **15** [500 MHz, $CDCl_3$].

Figure S19. Proposed mechanism for the intramolecular cycloetherification of *ε*–hydroxy–*α*,*β*–unsaturated ketones.

Figure S20. Phylogram of the most likely tree (–lnL = 10610.60) from a RAxML analysis of 116 taxa based on combined ITS and D1/D2 regions of LSU nrDNA sequence data (1052 bp).

Table S1. Crystal data, data collection, and refinement details

Tak1–TAB1 (Transforming growth factor–*β* activated kinase–1/TAK–1 binding protein 1) Inhibitor Assays.

The assay was performed using Kinase–Glo Plus luminescence kinase assay kit (Promega). It measures kinase activity by quantitating the amount of ATP remaining in solution following a kinase reaction. The luminescent signal from the assay is correlated with the amount of ATP present and is inversely correlated with the amount of kinase activity. Compounds (**1**–**14**) were diluted in 10% DMSO and 5 μL of the dilution was added to a 50 μL reaction so that the final concentration of DMSO is 1% in all of reactions. The compounds were preincubated with the enzyme in a reaction mixture for 10 min at room temperature. The enzymatic reactions were initiated by adding ATP (20 μM at final) and conducted for 40 min at 30 ^{o}C. The 50 μL reaction mixture contained 40 mM Tris, pH 7.4, 10 mM $MgCl_2$, 0.1 mg/mL BSA, 1 mM DTT, 0.2 mg/mL MBP substrate, 20 μM ATP and Tak1–TAB1. After the enzymatic reaction, 50 μL of Kinase–Glo Plus Luminescence kinase assay solution (Promega) was added to each reaction, and the plate was incubated for 20 min at room temperature. Luminescence signal was measured using a BioTek *Synergy 2* microplate reader. Tak1–TAB1 activity assays were performed in duplicate at each concentration. The luminescence data were analyzed using the computer software, Graphpad Prism. The difference between luminescence intensities in the absence of Tak1–TAB1 (Lu_t) and in the presence of Tak1–TAB1 (Lu_c) was defined as 100% activity ($Lu_t - Lu_c$). Using luminescence signal (Lu) in the presence of the compound, % activity was calculated as: % activity = $[(Lu_t - Lu)/(Lu_t - Lu_c)]\times 100\%$, where Lu= the luminescence intensity in the presence of the compound. The values of % activity versus a series of compound concentrations were then plotted using non–linear regression analysis of Sigmoidal dose–response curve generated with the equation $Y=B+(T-B)/1+10^{((LogEC50-X)\times Hill\ Slope)}$, where Y = percent activity, B = minimum percent activity, T = maximum percent activity, X = logarithm of compound and Hill Slope = slope factor or Hill coefficient. The IC_{50} values were determined by the concentration causing a half–maximal percent activity. 5*Z*–7–oxozeaenol was used as a positive control and showed an IC_{50} value of 21 nM.

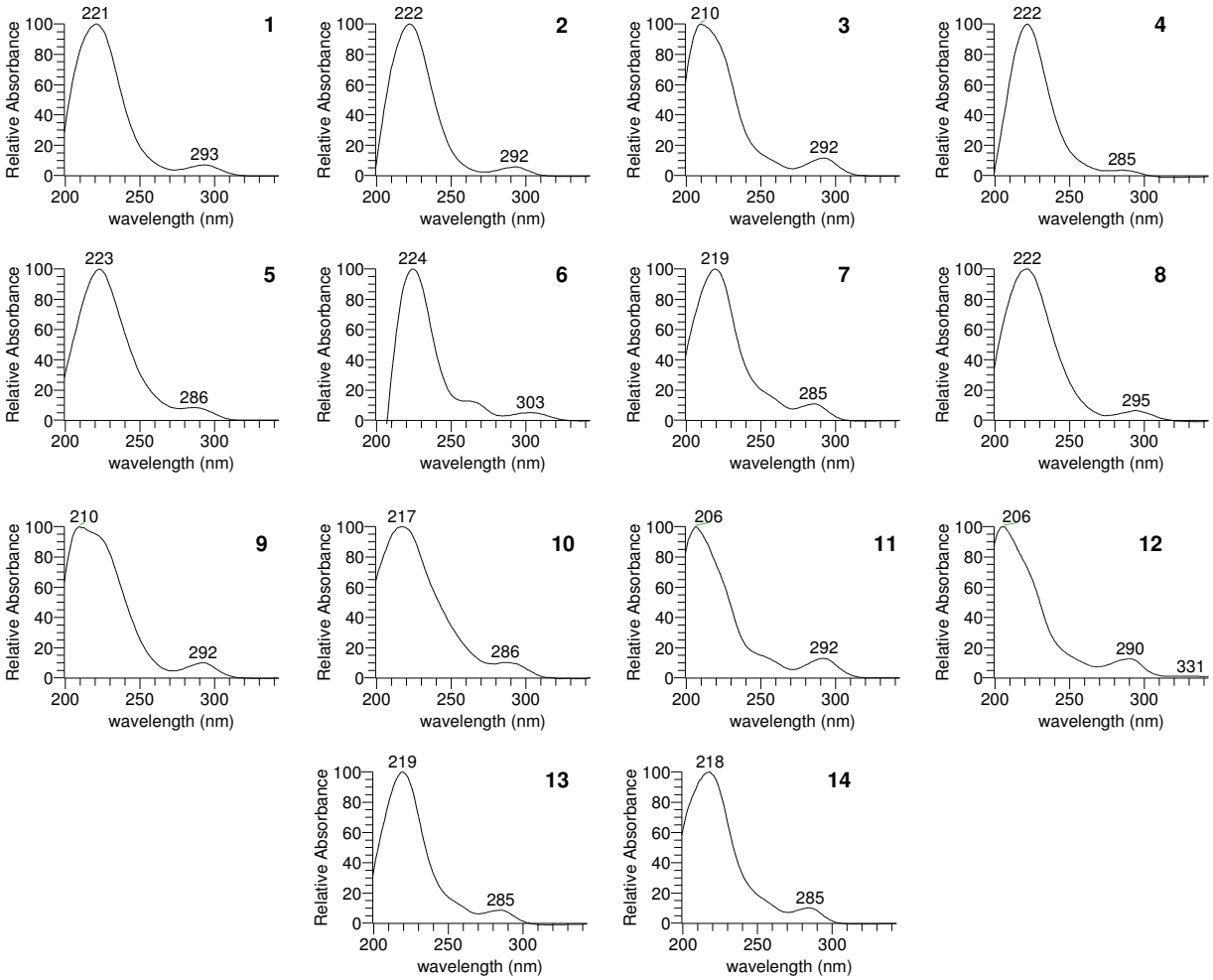

Figure S1. UV-PDA spectra of compounds **1**-**14** (200–345 nm).

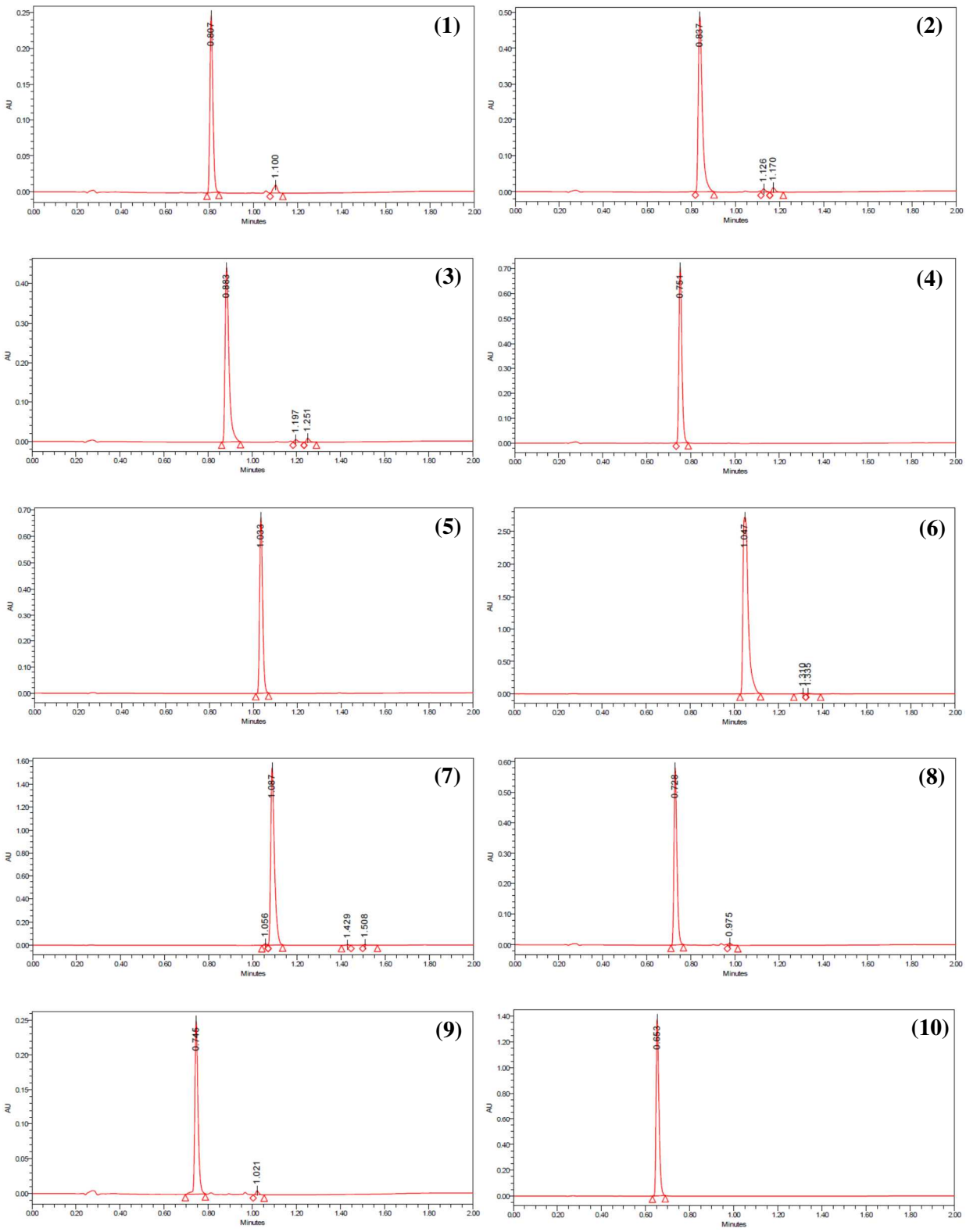
(1)
0.807
1.100
(2)
0.837
1.126
1.170
(3)
0.883
1.197
1.251
(4)
0.761
(5)
1.033
(6)
1.047
1.310
1.338
(7)
1.087
1.056
1.429
1.508
(8)
0.728
0.975
(9)
0.745
1.021
(10)
0.663
AU
Minutes

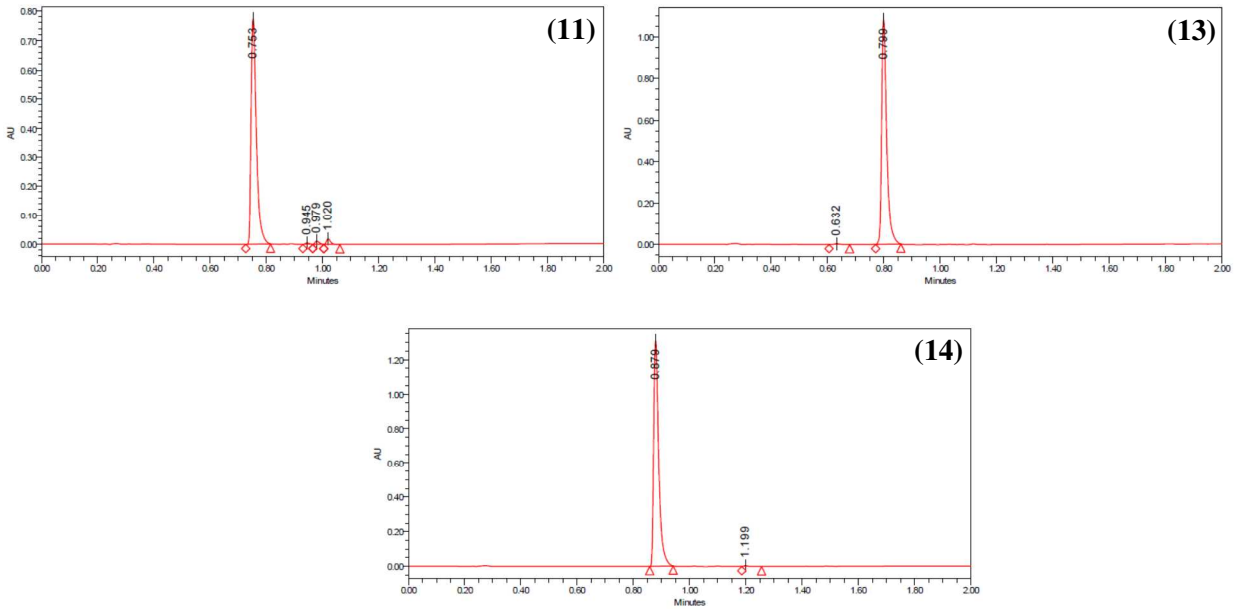

Figure S2. UPLC chromatograms of compounds **1–11** and **13–14** (λ 254 nm), demonstarting >96% purity for compounds **2–11** and **13–14** and >94% for compound **1**. All data were acquired via an Acquity UPLC system with a Phenomenex Kinetex C_{18} (1.3 μm; 50 × 2.1 mm) column and a CH_3CN/H_2O gradient that increased linearly from 20 to 100% CH_3CN over 1.2 min.

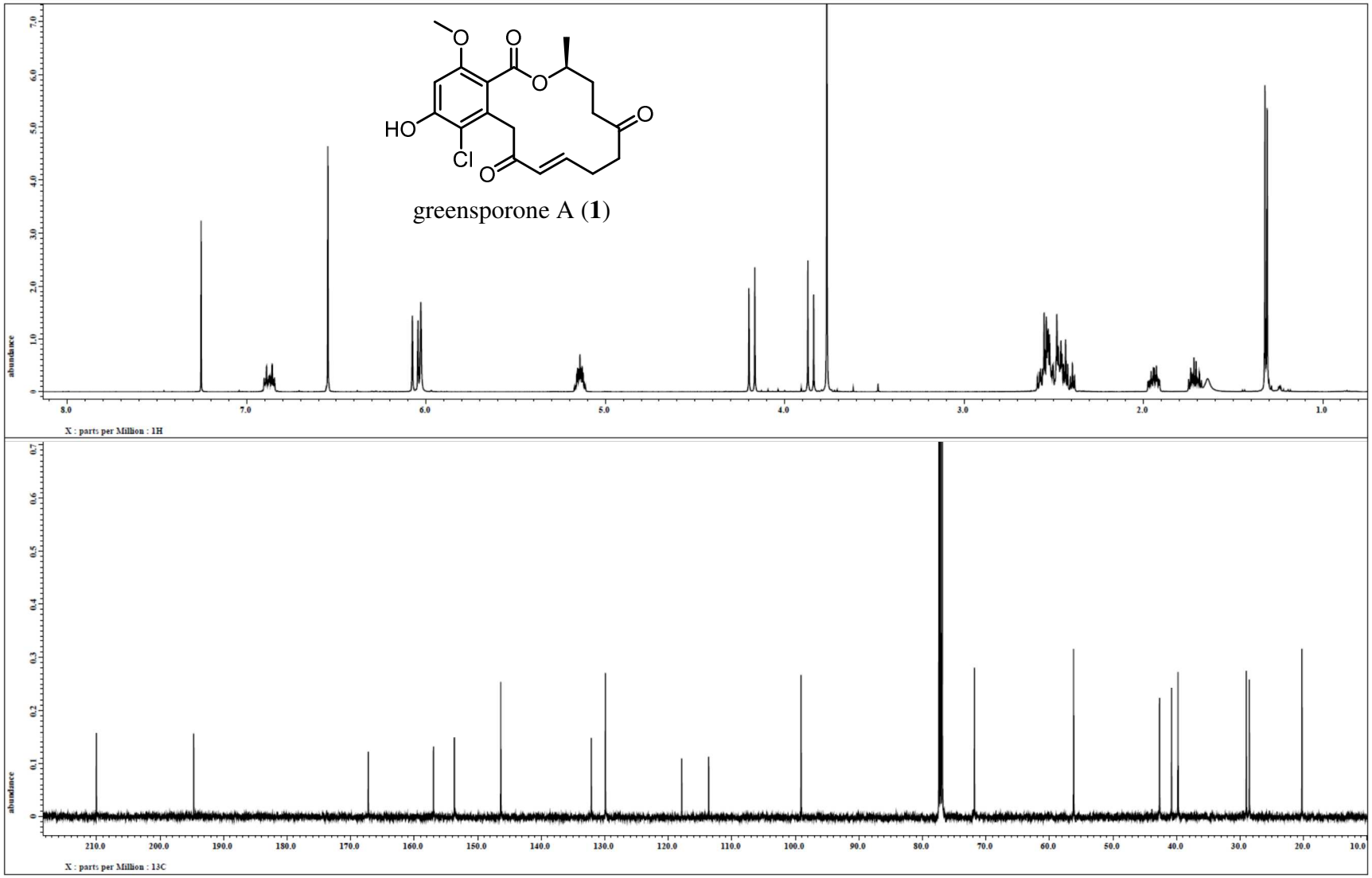

Figure S3. ^{1}H and ^{13}C NMR spectra of compound **1** [500 MHz for ^{1}H and 125 MHz for ^{13}C, $CDCl_3$].

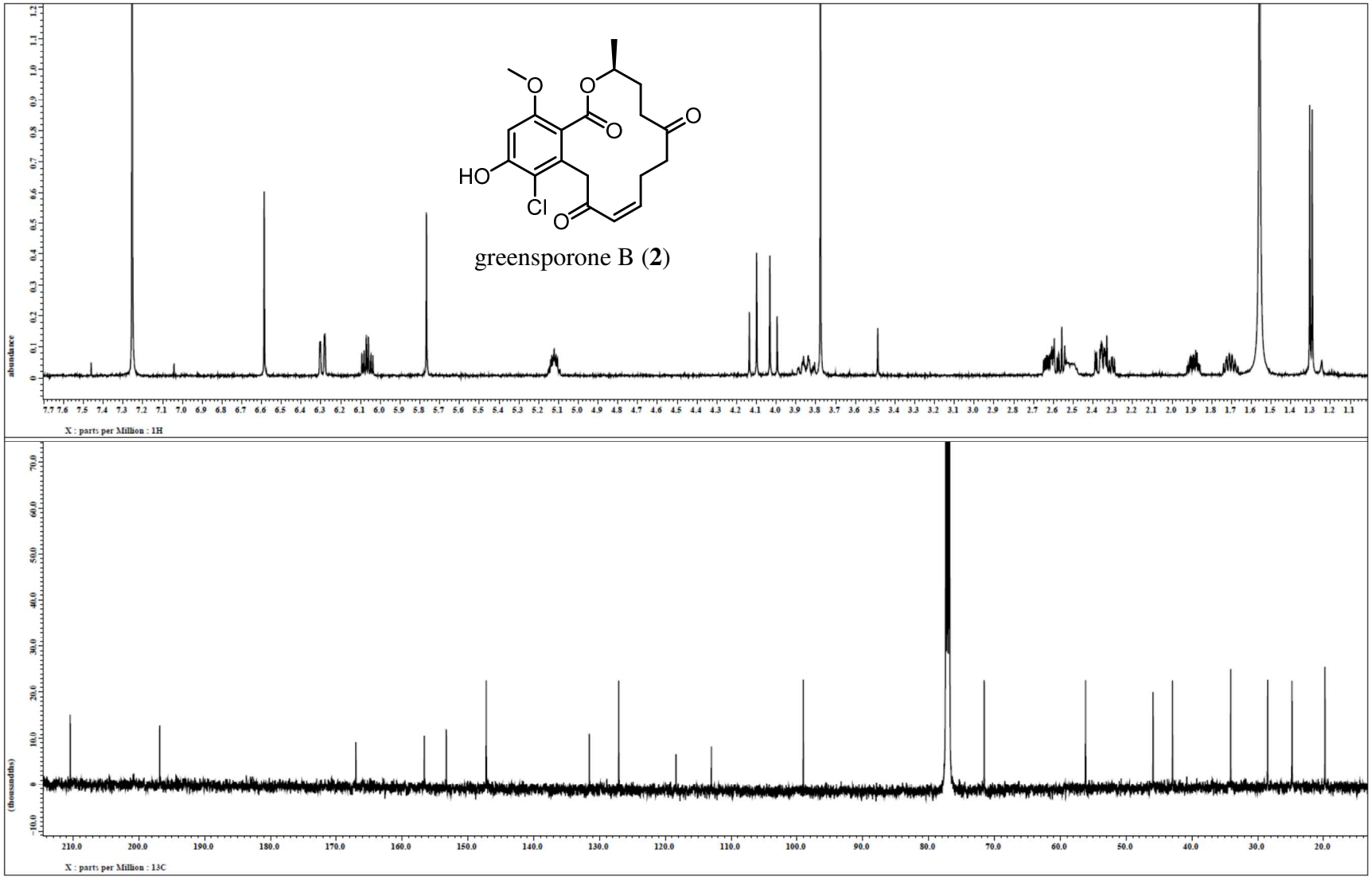

Figure S4. ^{1}H and ^{13}C NMR spectra of compound **2** [500 MHz for ^{1}H and 125 MHz for ^{13}C, $CDCl_3$].

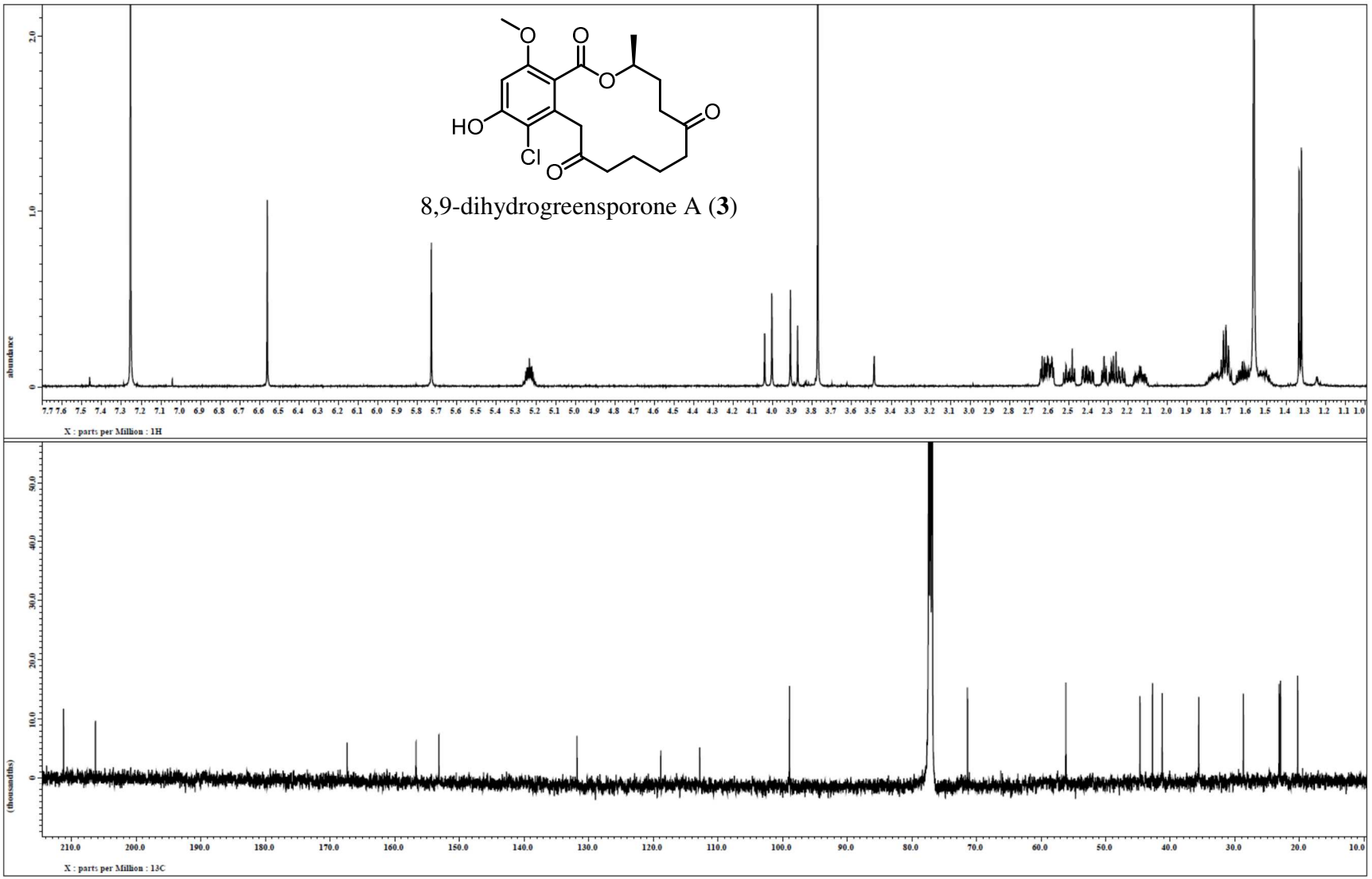

Figure S5. ^{1}H and ^{13}C NMR spectra of compound **3** [500 MHz for ^{1}H and 125 MHz for ^{13}C, $CDCl_3$].

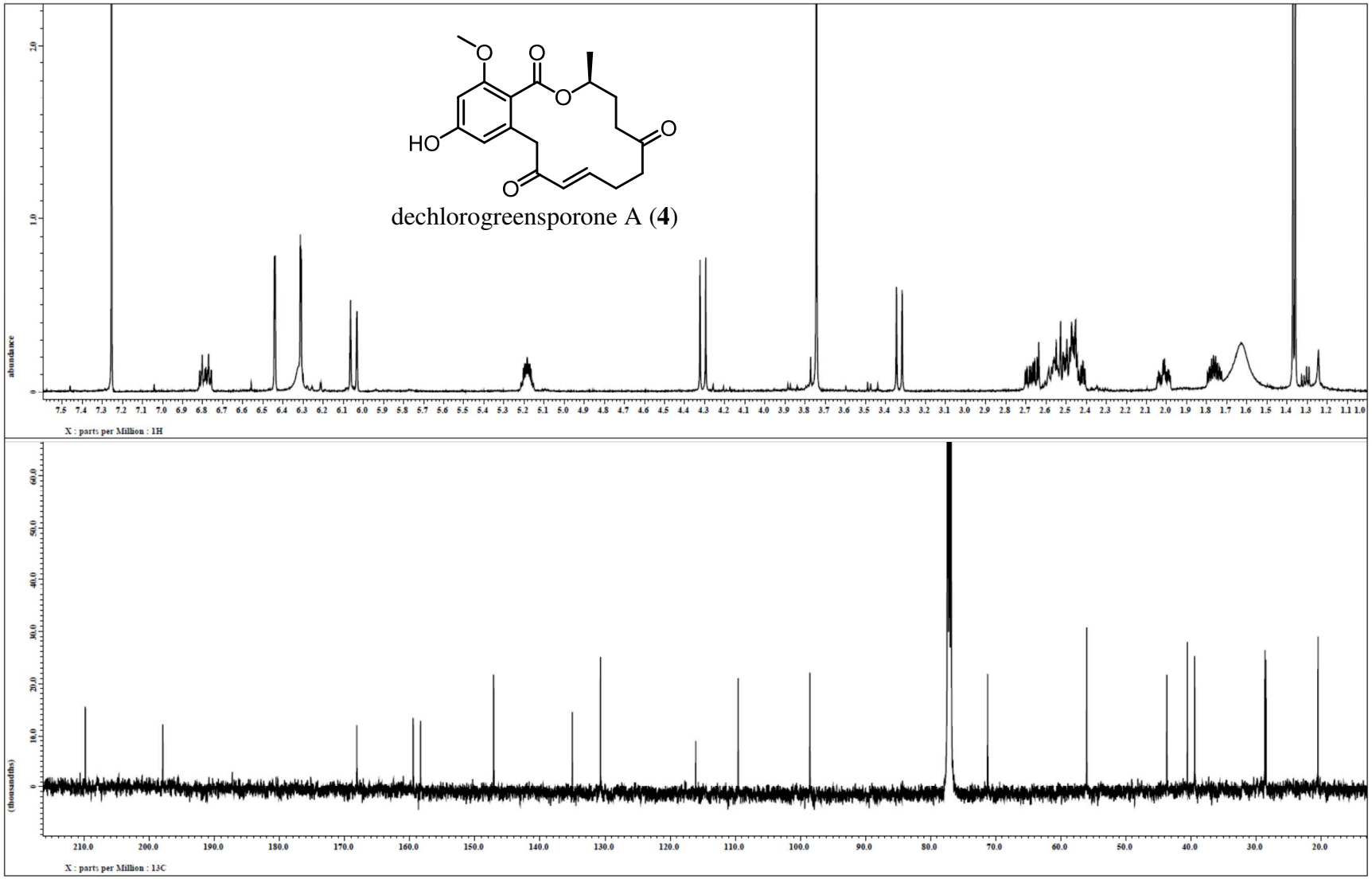

Figure S6. ^{1}H and ^{13}C NMR spectra of compound **4** [500 MHz for ^{1}H and 125 MHz for ^{13}C, $CDCl_3$].

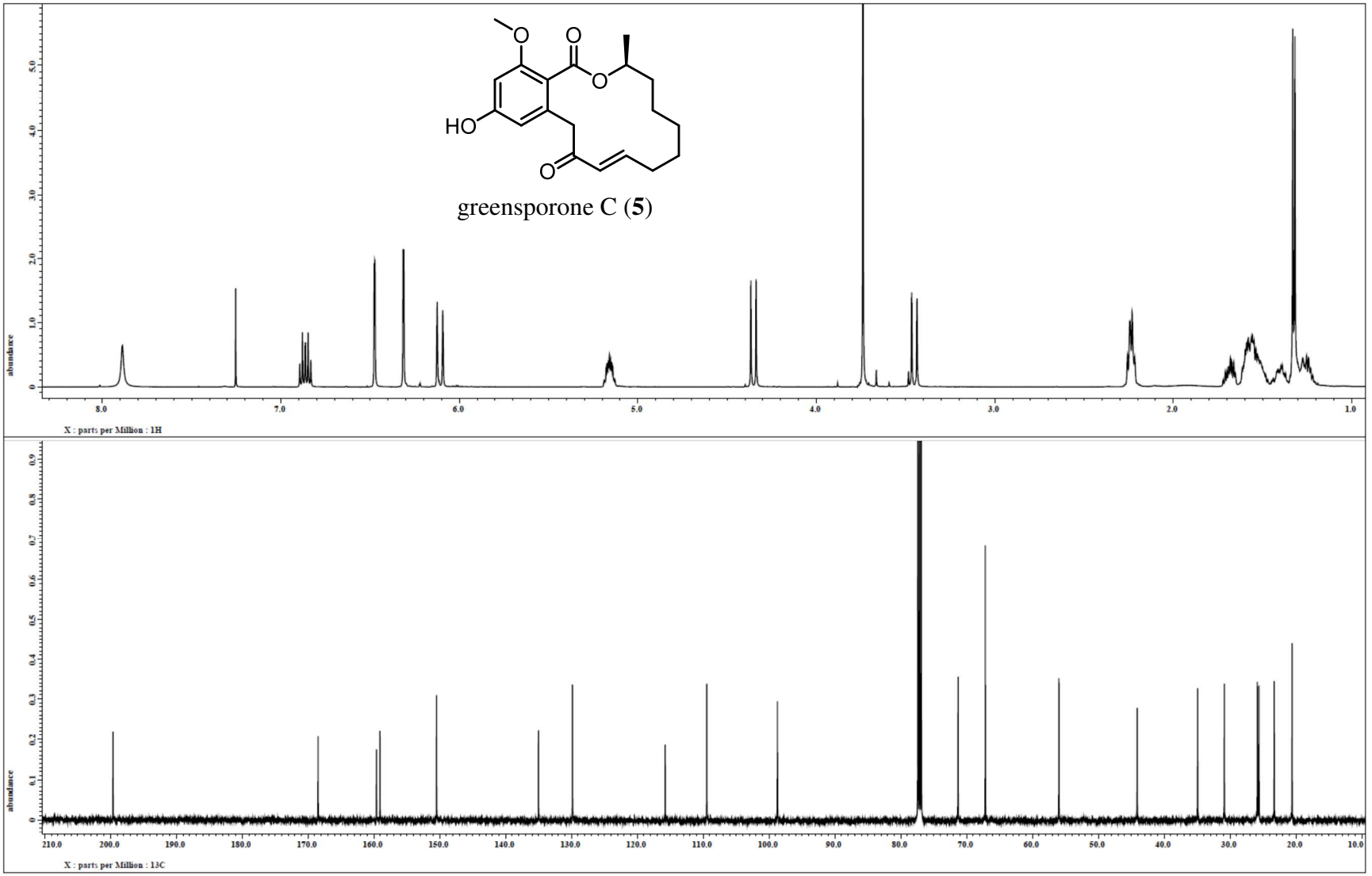

Figure S7. ^{1}H and ^{13}C NMR spectra of compound **5** [500 MHz for ^{1}H and 125 MHz for ^{13}C, $CDCl_3$].

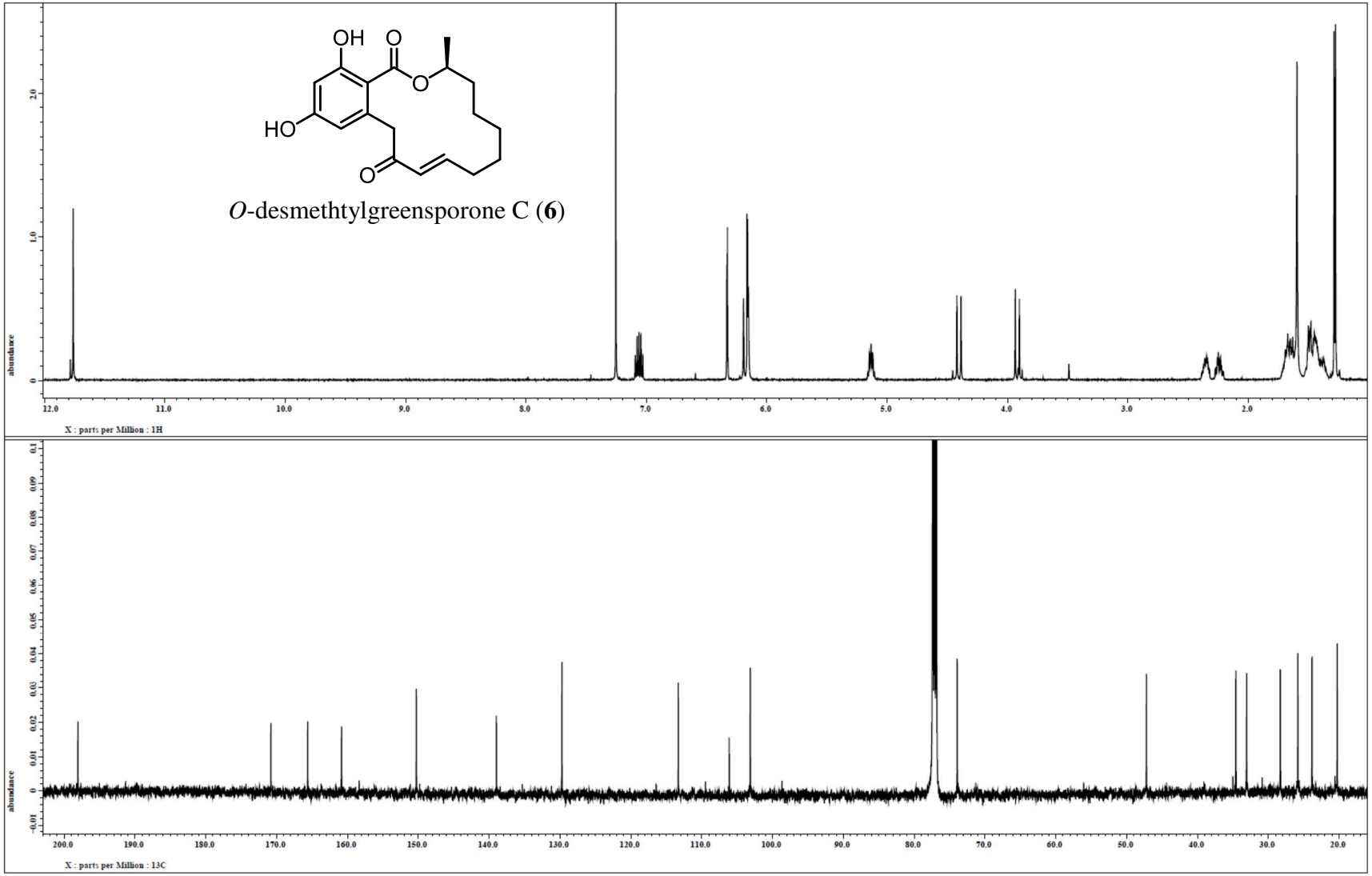

Figure S8. ^{1}H and ^{13}C NMR spectra of compound **6** [500 MHz for ^{1}H and 125 MHz for ^{13}C, $CDCl_3$].

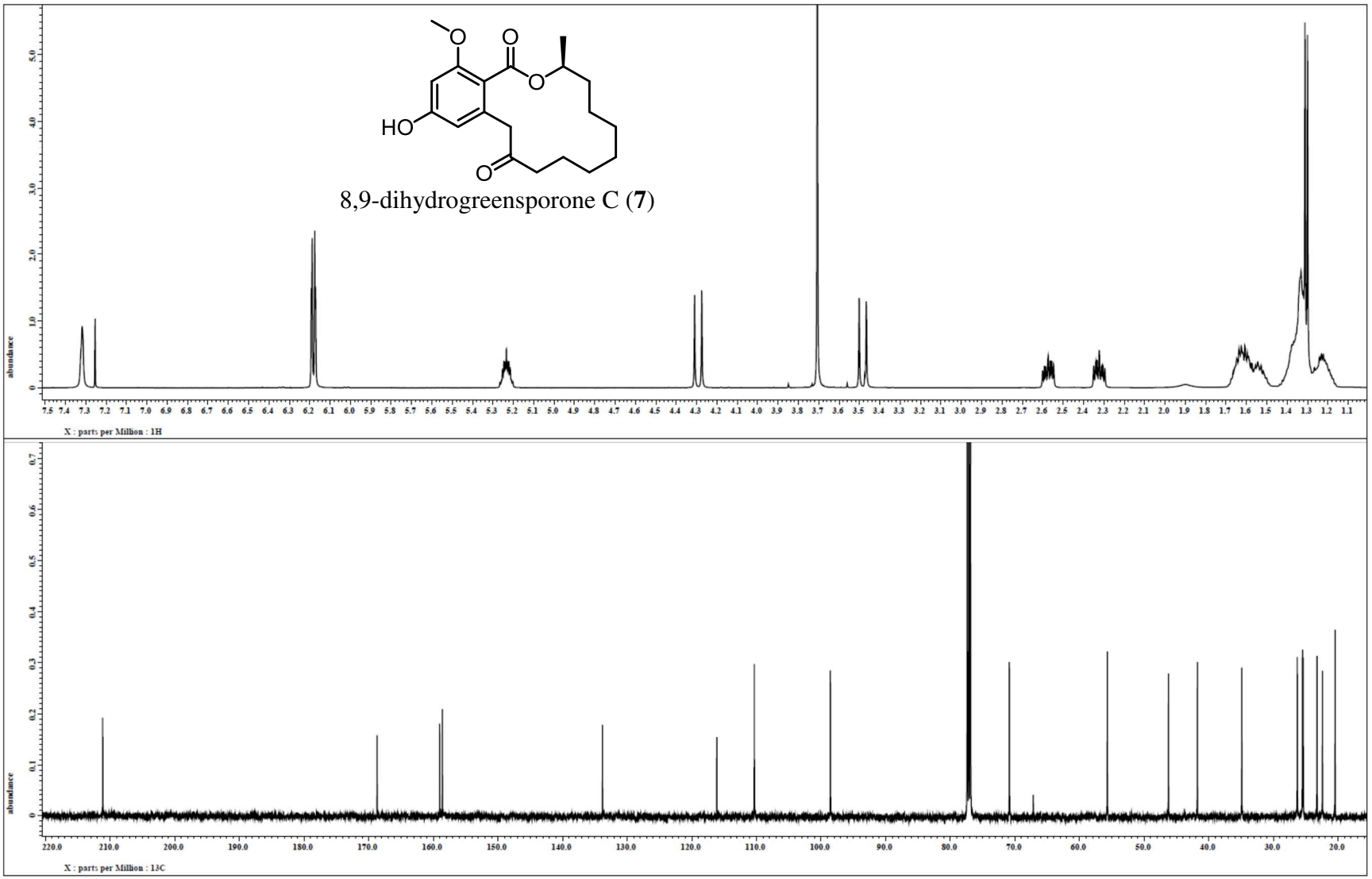

Figure S9. ^{1}H and ^{13}C NMR spectra of compound **7** [500 MHz for ^{1}H and 125 MHz for ^{13}C, $CDCl_3$].

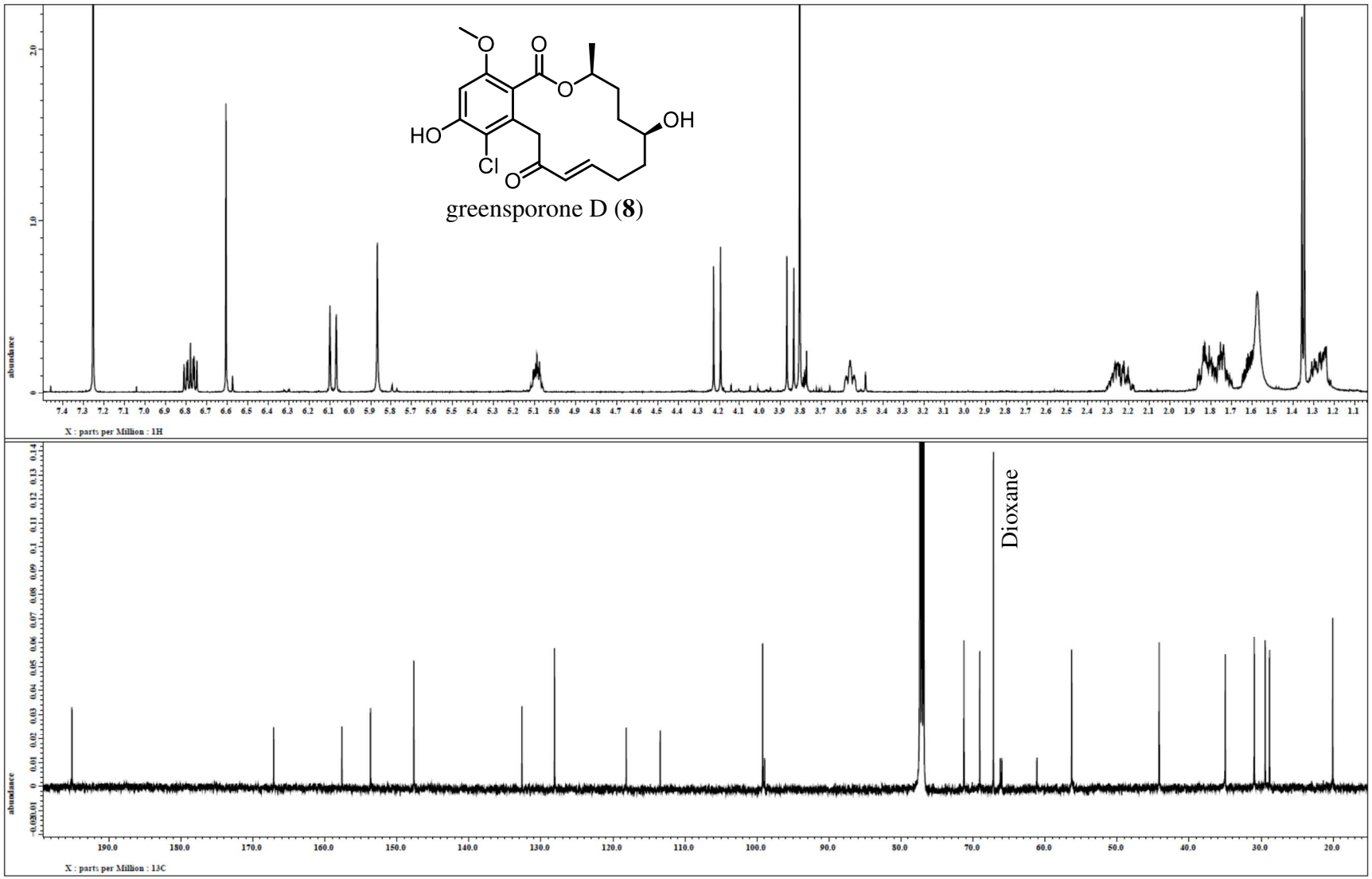

Figure S10. ^{1}H and ^{13}C NMR spectra of compound **8** [500 MHz for ^{1}H and 125 MHz for ^{13}C, $CDCl_3$].

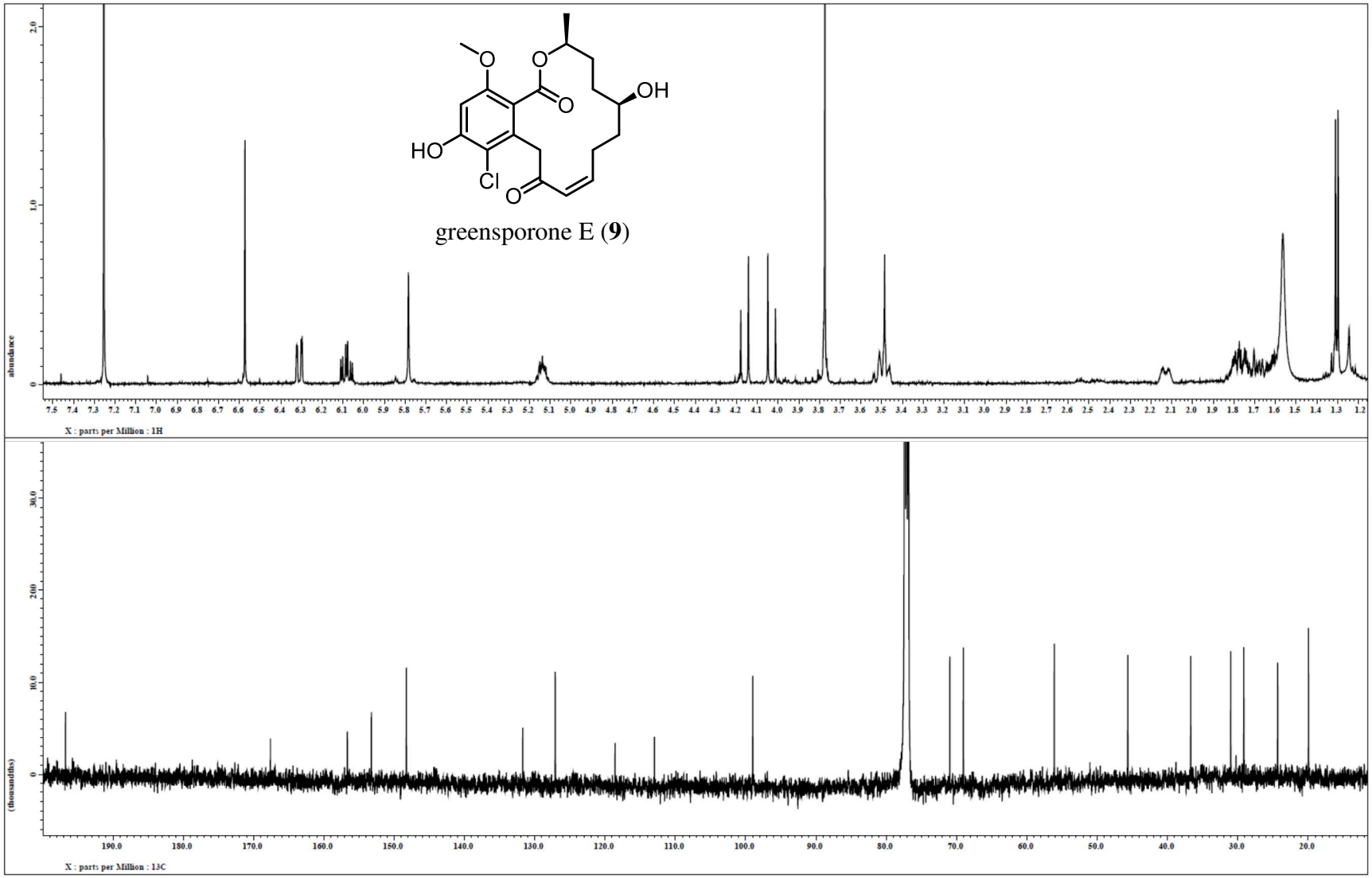

Figure S11. ^{1}H and ^{13}C NMR spectra of compound **9** [500 MHz for ^{1}H and 125 MHz for ^{13}C, $CDCl_3$].

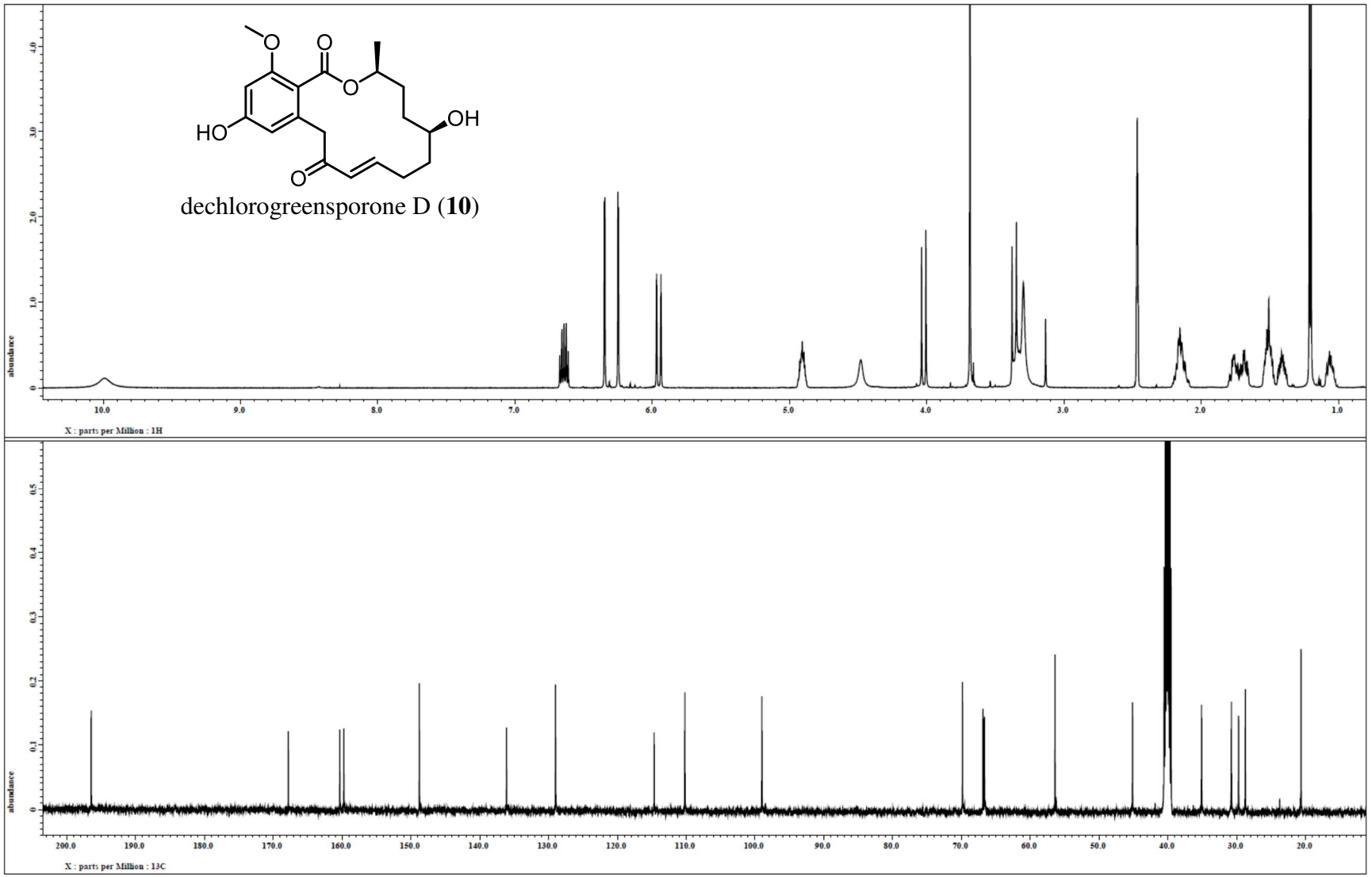

Figure S12. ^{1}H and ^{13}C NMR spectra of compound **10** [500 MHz for ^{1}H and 125 MHz for ^{13}C, DMSO].

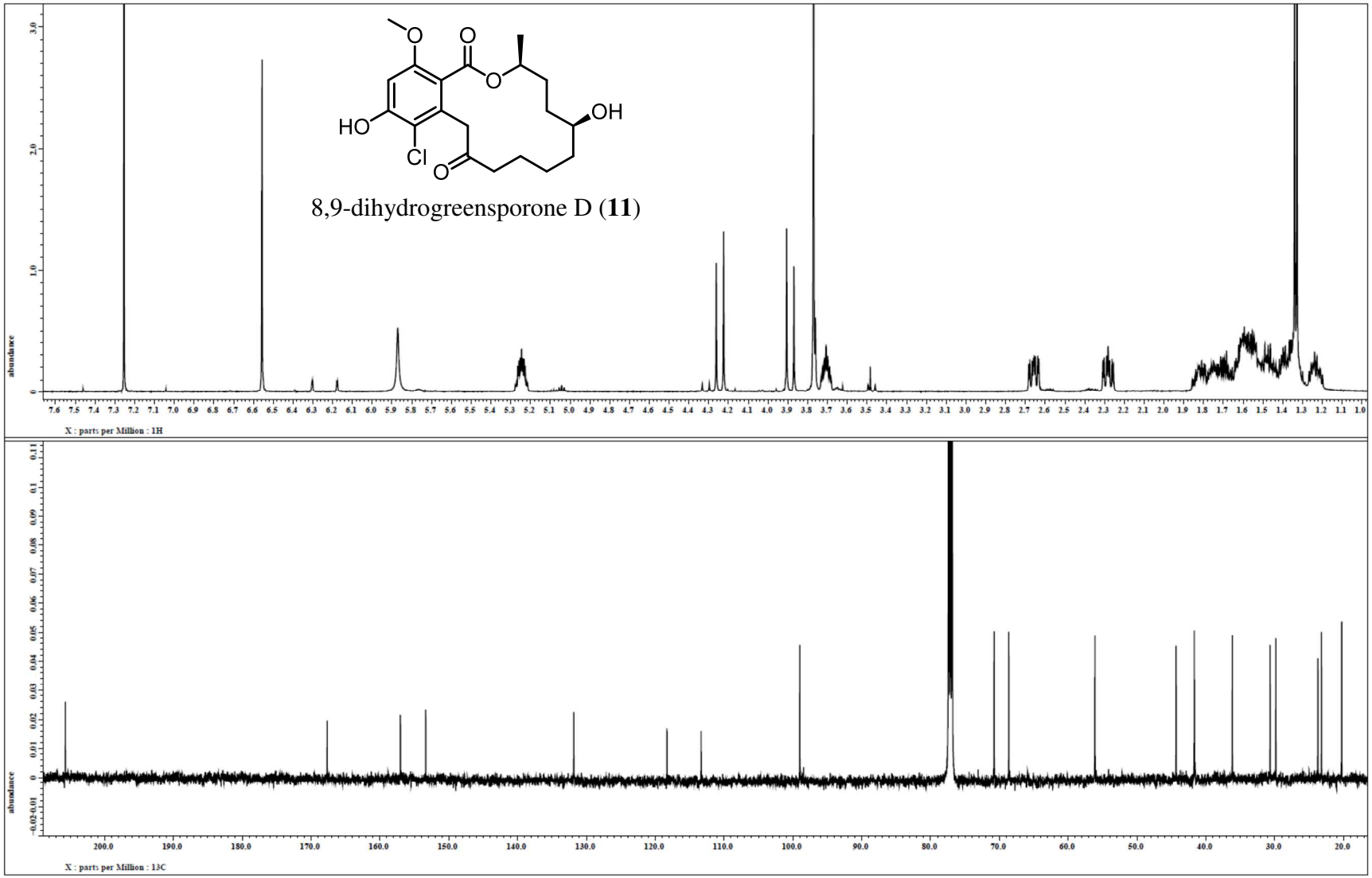

Figure S13. ^{1}H and ^{13}C NMR spectra of compound **11** [500 MHz for ^{1}H and 125 MHz for ^{13}C, $CDCl_3$].

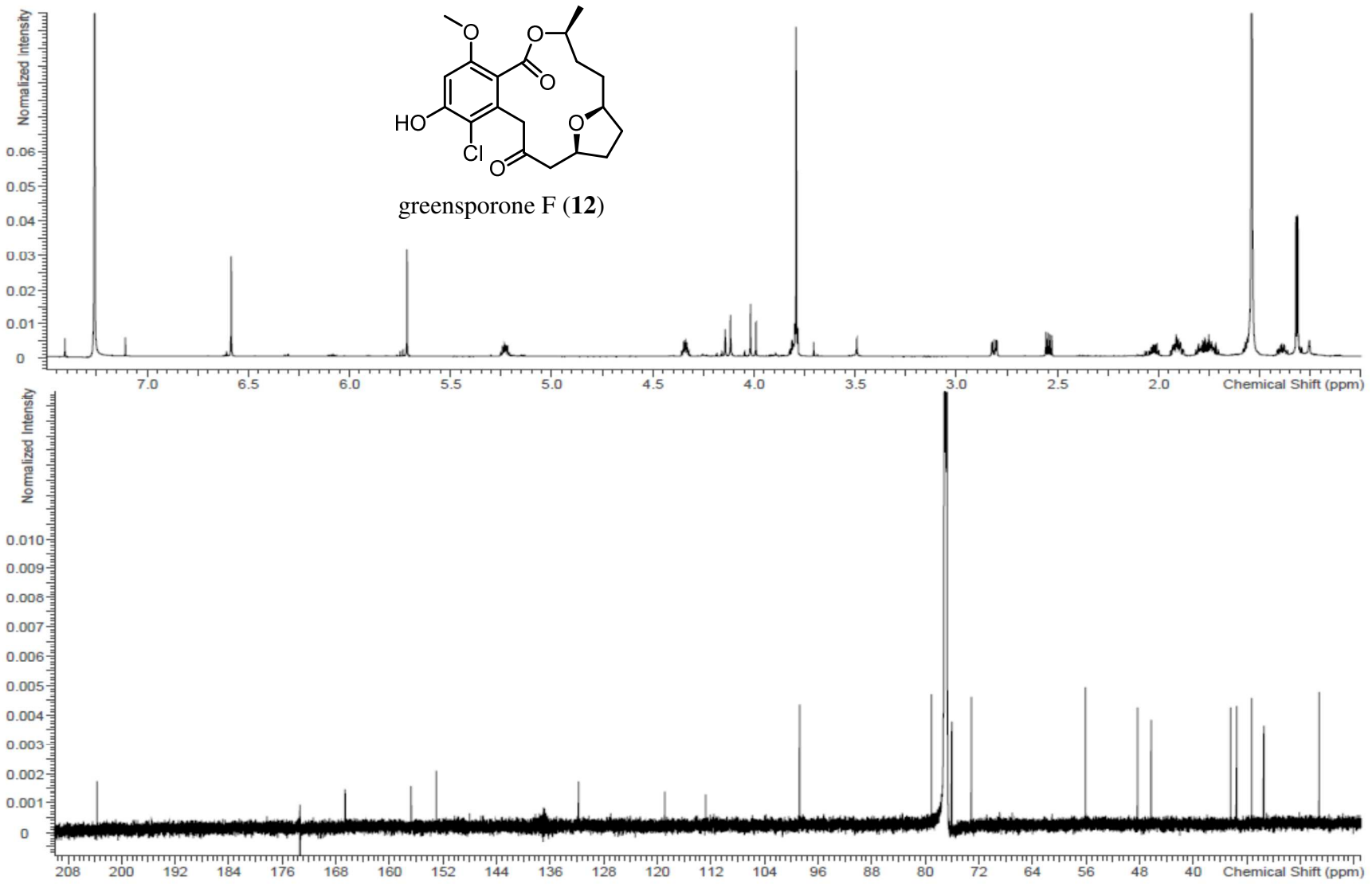

Figure S14. ^{1}H and ^{13}C NMR spectra of compound **12** [700 MHz for ^{1}H and 175 MHz for ^{13}C, $CDCl_3$].

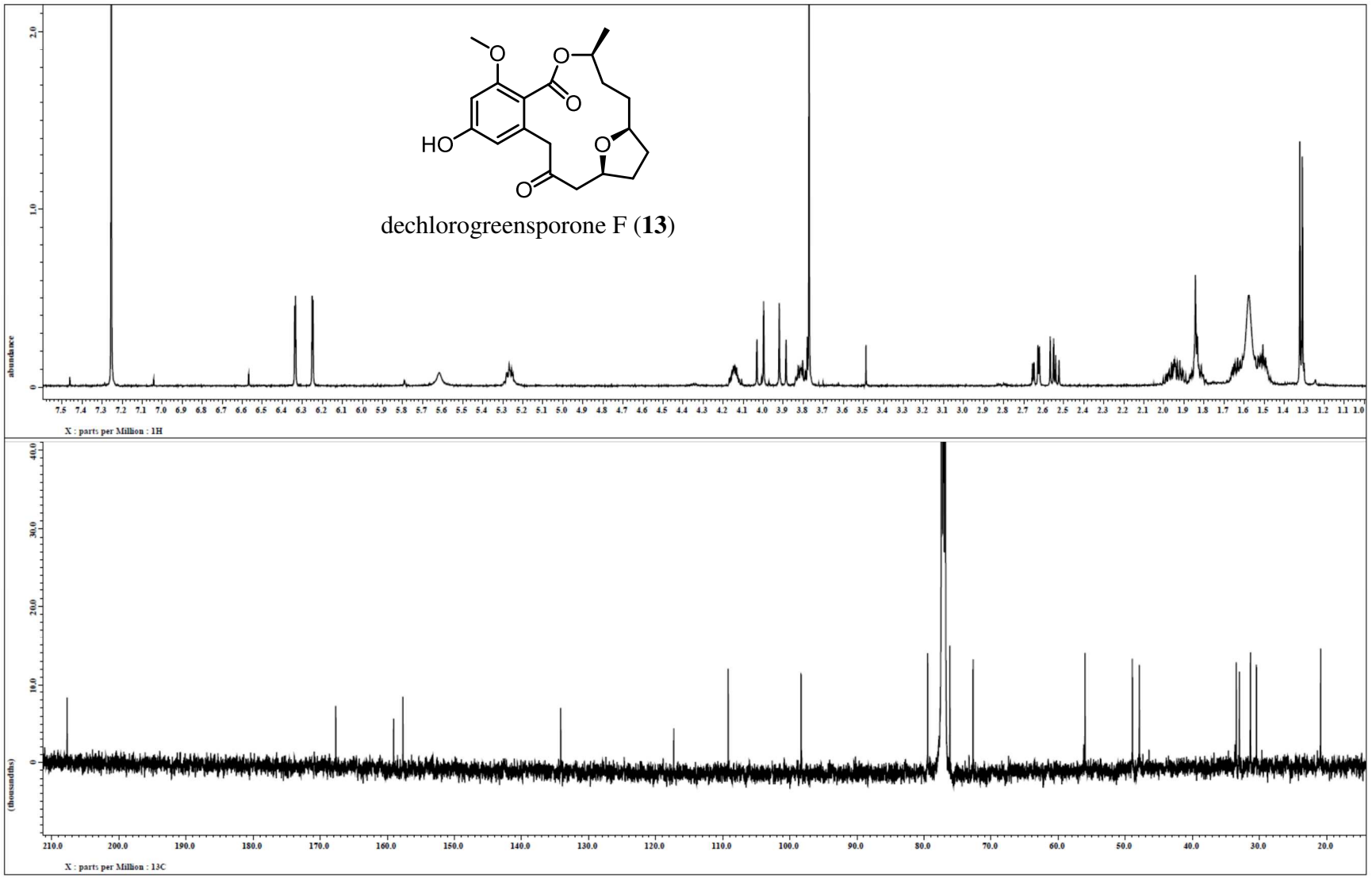

Figure S15. ^{1}H and ^{13}C NMR spectra of compound **13** [500 MHz for ^{1}H and 125 MHz for ^{13}C, $CDCl_3$].

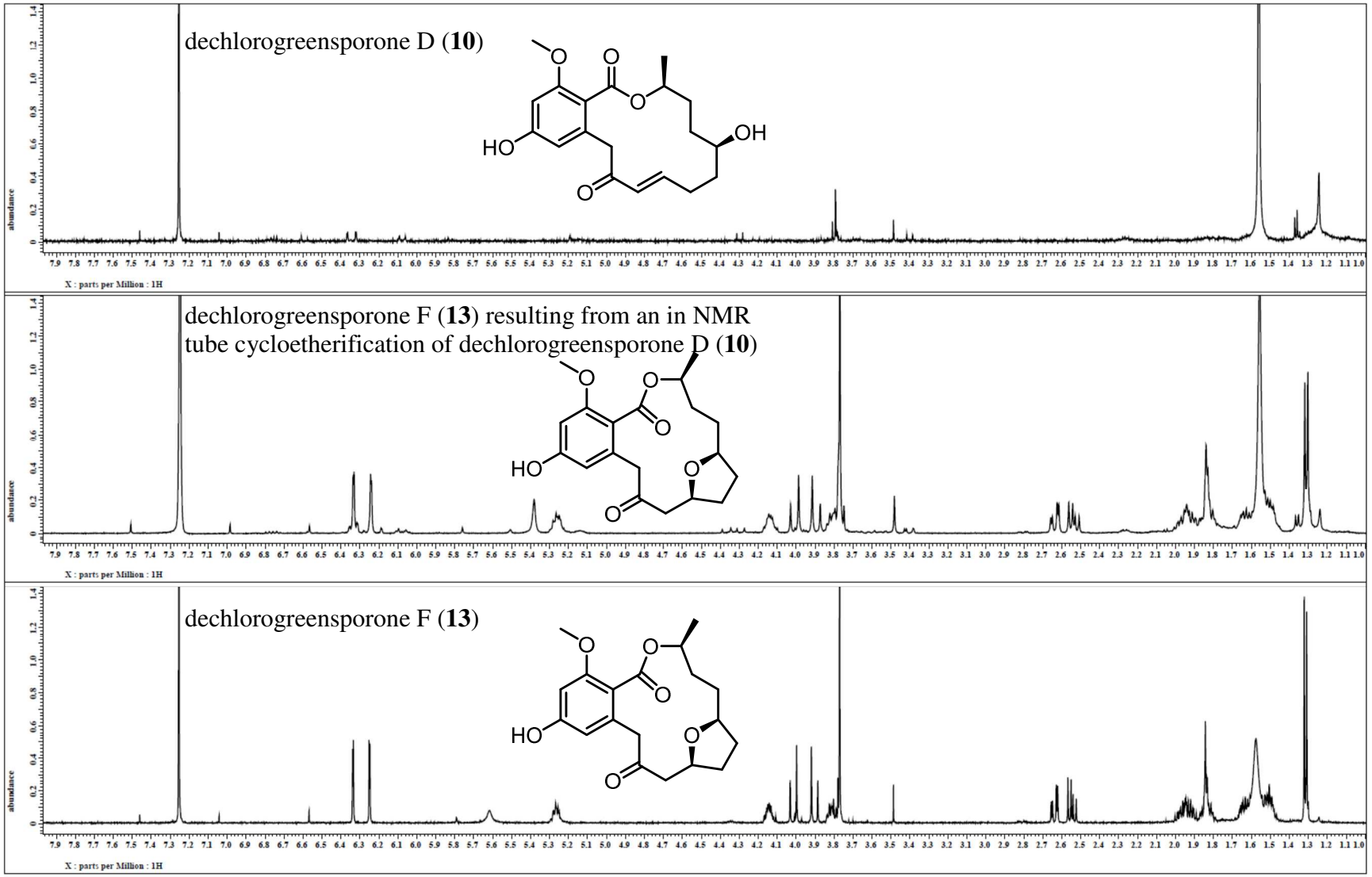

Figure S16. Stack plot of the ^{1}H NMR spectra of compound **10** (upper), compound **13** (lower) and the rearranged product of compound **10** (middle) [500 MHz, $CDCl_3$].

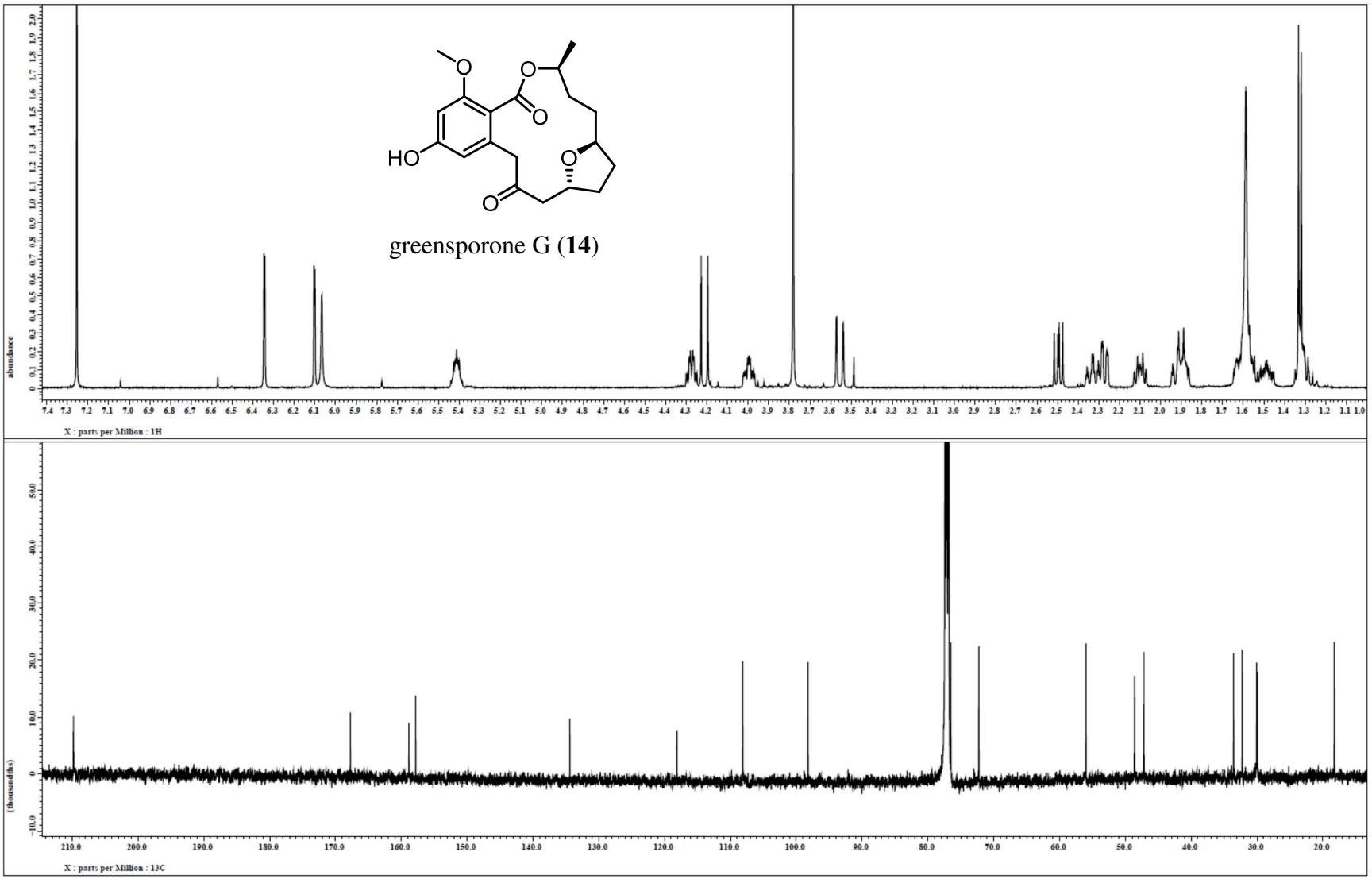

Figure S17. ^{1}H and ^{13}C NMR spectra of compound **14** [500 MHz for ^{1}H and 125 MHz for ^{13}C, $CDCl_3$].

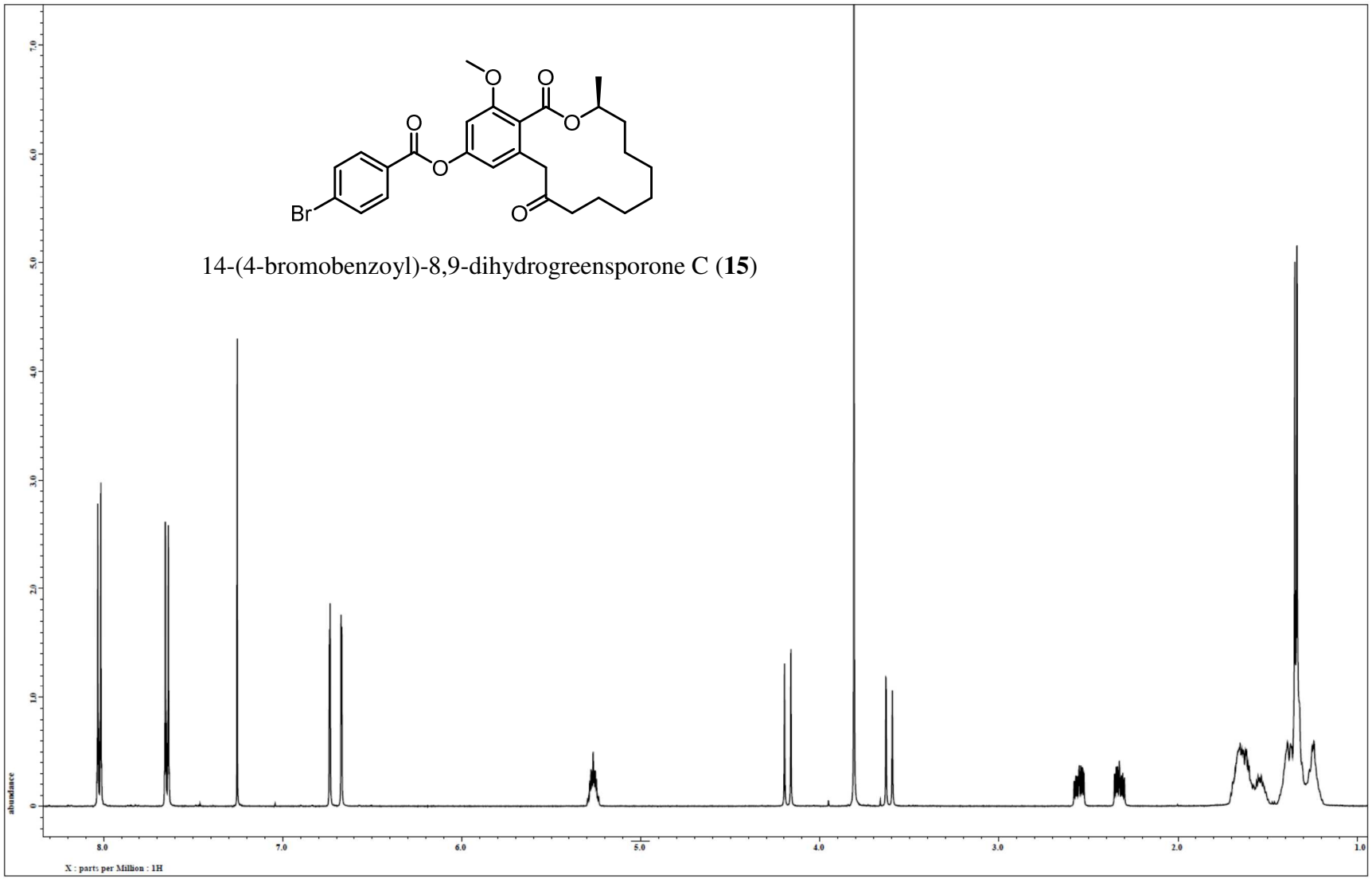

Figure S18. ^{1}H NMR spectrum of compound **15** [500 MHz, $CDCl_3$].

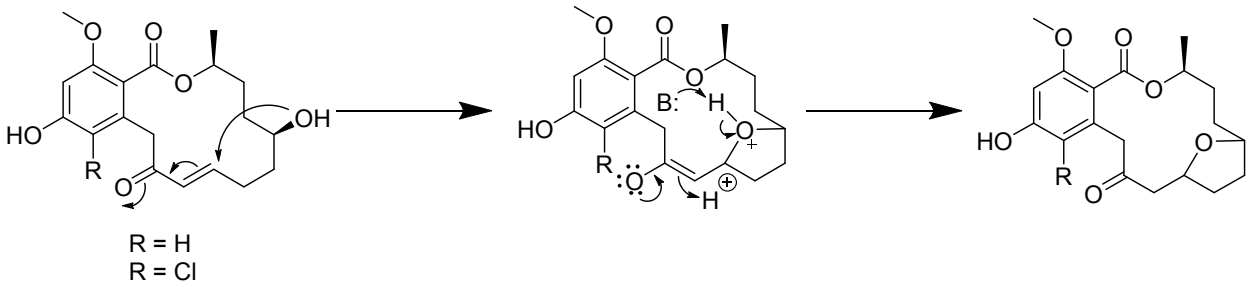

Figure S19. Proposed mechanism for the intramolecular cycloetherification of *ε*–hydroxy–*α*,*β*–unsaturated ketones.

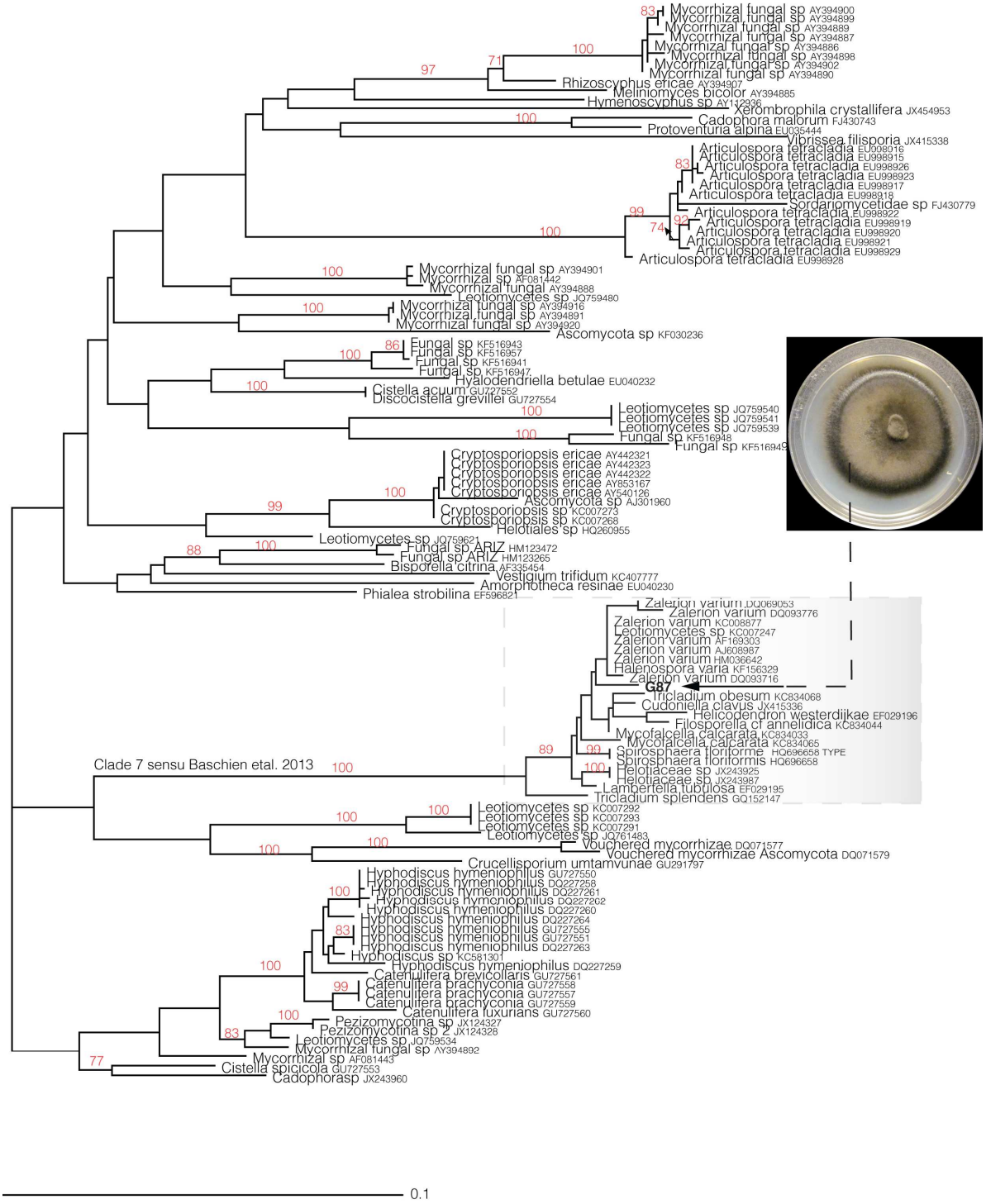

Figure S20. Phylogram of the most likely tree (–lnL = 10610.60) from a RAxML analysis of 116 taxa based on combined ITS and D1/D2 regions of LSU nrDNA sequence data (1052 bp). Numbers refer to RAxML bootstrap support values ≥ 70% based on 1000 replicates. Strain G87 was putatively identified as having phylogenetic affinities to *Halenospora varia* (Clade 7 sensu Baschien et al. 2013 highlighted). Bar indicates nucleotide substitution per site. A 3–week–old colony of G87 on PDA media is also shown.

Table S1. Crystal data, data collection, and refinement details

Crystal data	
$C_{26}H_{29}BrO_6$	$F(000) = 1072$
$M_r = 517.40$	$D_x = 1.395$ Mg m^{-3}
Monoclinic, $C2$	Mo $K\alpha$ radiation, $\lambda = 0.71073$ Å
$a = 22.9481$ (11) Å	Cell parameters from 9887 reflections
$b = 5.2631$ (3) Å	$\theta = 3.6$–$30.9°$
$c = 21.5301$ (11) Å	$\mu = 1.71$ mm^{-1}
$\beta = 108.6665$ (6)°	$T = 193$ K
$V = 2463.6$ (2) Å^3	Rectangular–parallepiped, colourless
$Z = 4$	$0.52 \times 0.19 \times 0.12$ mm
Data collection	
Bruker APEX CCD diffractometer	7231 independent reflections
Radiation source: sealed tube	6524 reflections with $I > 2\sigma(I)$
Graphite monochromator	$R_{int} = 0.031$
ϕ and ω scans	$\theta_{max} = 30.2°$, $\theta_{min} = 3.6°$
Absorption correction: multi–scan; Data were corrected for scaling and absorption effects using the multi–scan technique (*SADABS*). The ratio of minimum to maximum apparent transmission was 0.774. The calculated minimum and maximum transmission coefficients (based on crystal size) are 0.471 and 0.821.	$h = -32 \rightarrow 32$
$T_{min} = 0.577$, $T_{max} = 0.746$	$k = -7 \rightarrow 7$
23715 measured reflections	$l = -30 \rightarrow 30$
Refinement	
Refinement on F^2	Secondary atom site location: structure–invariant direct methods
Least–squares matrix: full	Hydrogen site location: inferred from neighbouring sites
$R[F^2 > 2\sigma(F^2)] = 0.037$	H–atom parameters constrained
$wR(F^2) = 0.096$	$w = 1/[\sigma^2(F_o^2) + (0.0457P)^2 + 2.0649P]$ where $P = (F_o^2 + 2F_c^2)/3$
$S = 1.03$	$(\Delta/\sigma)_{max} = 0.001$
7231 reflections	$\Delta\rangle_{max} = 1.23$ e Å^{-3}

300 parameters	$\Delta\rangle_{min} = -0.81$ e Å^{-3}
1 restraint	Absolute structure: Flack x determined using 2675 quotients [(I+)-(I-)]/[(I+)+(I-)] (Parsons and Flack (2004), Acta Cryst. A60, s61).
Primary atom site location: structure–invariant direct methods	Absolute structure parameter: –0.011 (3)